

HENRY

Hydraulic Engineering Repository

Ein Service der Bundesanstalt für Wasserbau

Conference Paper, Published Version

Tominaga, Akihiro; Hashimoto, Naohiko; Liu, Jian

Experimental Study on Three-Dimensional Flow Structures in Straight River Channel with a Pool

Zur Verfügung gestellt in Kooperation mit/Provided in Cooperation with:
Kuratorium für Forschung im Küsteningenieurwesen (KFKI)

Verfügbar unter/Available at: <https://hdl.handle.net/20.500.11970/110224>

Vorgeschlagene Zitierweise/Suggested citation:

Tominaga, Akihiro; Hashimoto, Naohiko; Liu, Jian (2008): Experimental Study on Three-Dimensional Flow Structures in Straight River Channel with a Pool. In: Wang, Sam S. Y. (Hg.): ICHE 2008. Proceedings of the 8th International Conference on Hydro-Science and Engineering, September 9-12, 2008, Nagoya, Japan. Nagoya: Nagoya Hydraulic Research Institute for River Basin Management.

Standardnutzungsbedingungen/Terms of Use:

Die Dokumente in HENRY stehen unter der Creative Commons Lizenz CC BY 4.0, sofern keine abweichenden Nutzungsbedingungen getroffen wurden. Damit ist sowohl die kommerzielle Nutzung als auch das Teilen, die Weiterbearbeitung und Speicherung erlaubt. Das Verwenden und das Bearbeiten stehen unter der Bedingung der Namensnennung. Im Einzelfall kann eine restriktivere Lizenz gelten; dann gelten abweichend von den obigen Nutzungsbedingungen die in der dort genannten Lizenz gewährten Nutzungsrechte.

Documents in HENRY are made available under the Creative Commons License CC BY 4.0, if no other license is applicable. Under CC BY 4.0 commercial use and sharing, remixing, transforming, and building upon the material of the work is permitted. In some cases a different, more restrictive license may apply; if applicable the terms of the restrictive license will be binding.

EXPERIMENTAL STUDY ON THREE-DIMENSIONAL FLOW STRUCTURES IN STRAIGHT RIVER CHANNEL WITH A POOL

Akihiro TOMINAGA¹, Naohiko HASHIMOTO² and Jian LIU³

¹ Professor, Department of Civil Engineering, Nagoya Institute of Technology, Gokiso-cho, Showa-ku, Nagoya 466-8555, Japan, e-mail: tominaga.akihiro@nitech.ac.jp

² CTI Engineering Co., Ltd., 1-14-6, Kamikizaki, Urawa-ku, Saitama, 330-0071, Japan

³ Associate Professor, College of Civil Engineering, Shenzhen University, Nanhai Ave 3688, Shenzhen, Guangdong, P.R.China, 518060, e-mail: liujian@szu.edu.cn

ABSTRACT

Pool-riffle sequences are important for improvement of habitats and restoration of channelized urban streams. However, their hydrodynamic behaviour has not yet fully understood to date. In this study, we pay attention to the flow characteristic of pool in pool-riffle sequence. The pool was made at fixed bed condition imitating actual river channel of mountain section. Three-dimensional flow structures in this open channel with a pool were analyzed by measuring three-dimensional velocities with electromagnetic velocimeters. A cylindrical separation vortex was generated in a deep pool zone on one side unexpectedly. When permeable groyne structures were set in the pool, the vortex in the pool was reduced in size and a new separation vortex appeared on the opposite side. The separation vortices were almost two-dimensional but secondary flows were observed in cross sections. The turbulence intensities were also dominated by the horizontal vortex structures.

Keywords: pool and riffle, flow structures, permeable groyne, separation vortices, turbulence

1. INTRODUCTION

Pool-riffle sequences are important configurations in natural rivers for ecological habitats of aquatic life. Recently, many pool configurations have been lost by river improvements for flood protection works or some artificial actions. Such deleterious changes in river configurations decrease habitats for wide variety of aquatic life. Restoration and creation of pool-riffle sequences become to be recognized as useful measures for ecological environments. In particular, the physical environment of pool configuration is an important factor for fish habitats. Generally, pools provide deep water-depth and low flow-velocity that is necessary for the life of some kind of fish. However, the flow structures in pools must be changed depending on the river flow rate. It is essential that pools should not be buried by deposition of sediment during high stage flow.

The studies on pool-riffle configuration were mainly concentrated on its effects on flow mixing or sediment transport in one-dimensional aspect (Seo et al.,1992 and Cui et al.,2008). There were a few researches on the flow structures in pool-riffle configurations. Since the flow behaviours in pools are three dimensional, it is not easy to design artificial pools. To create and maintain pools, it is necessary to investigate three-dimensional flow structures and bed deformation in channels with them. This type of flow is represented by the open channel flow over concavity on bed. Miyamoto et al. (2001) investigated the turbulent structure in open channel flow over bed concavity. However, this concavity zone was a rectangular shape and the separated flow was significant. As to the flow structures in pool-riffle sequence, Booker et al. (2002) and Rodriguez et al. (2004) studied change of near-bed

velocity and bed shear stress by flow rate and their effects on sediment transport.

Sometimes, void areas among stones are required for nesting and breeding. Stone nets or boulder blocks are often used for improving habitat environment. In this case, the effects of artificial structures on flow and sediment deposition should be predicted. In this study, we conducted a set of laboratory experiments in an open channel with an asymmetrical pool that is created on a straight river reach. In order to maintain pool configuration, permeable groynes were set in a deep pool zone. Three-dimensional velocities were measured and compared in a pool zone in the conditions with and without groynes.

2. EXPERIMENTAL METHODS

The experimental flume was 13m long, 0.6m wide and 0.3m high, slope-variable rectangular flume. An asymmetrical pool was configured by digging down the sand bed and hardened as shown in Figure 1. The upstream end of the pool zone was 7.3m downstream from the channel entrance. The length of the pool was 1.0m and the left-hand side deepest area was 0.6m long, 0.2m wide and 0.04m deep. The slope of upstream and downstream slants of the pool was 1/5, and the slope of side slant was 1/10. The slope of the channel was 0.00125. The water depth was controlled at 1m downstream from the pool end by adjusting downstream weir. The experimental conditions are shown in Table 1. This pool configuration was simply modelled with reference to the actual river and the expected scale was 1/50. The experimental discharge condition corresponds to about 50m³/s in prototype which is considered to be a medium-high flow condition. The case SP had no groynes and the case FP had two groynes in the deepest pool area. Rectangular box frames with slit were used to make groyne models as shown in Figure 2. By lading two box frames, the groyne model becomes 5cm x 5cm in the base plane and 6cm in height. Gravels with mean diameter of 7mm were filled in the box frame and its void rate was 0.50. These two sets of groyne model were located at 20cm and 40cm from the upstream edge of the deepest plane zone. The velocity was measured by I-type and L-type two-component electromagnetic velocimeters twice at the same points. Then two sets of velocities (u, v) and (u, w) were obtained and integrated to three components of velocity (u, v, w). The streamwise direction is x , transverse direction is y and vertical direction is z . The origin of x is set at the upstream edge of the pool configuration.

Table 1 Experimental conditions

CASE	Discharge Q (lit/s)	Flow depth Hs (cm)	Pool depth Hp (cm)	Mean velocity Um (cm/s)	Bed slope I
SP	2.92	2.3	6.3	21.9	0.00125
FP	2.71	2.4	6.4	18.7	0.00125

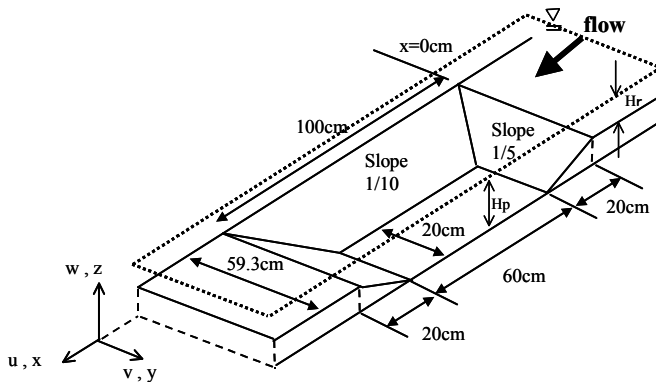


Figure 1 Schematic view of pool configuration

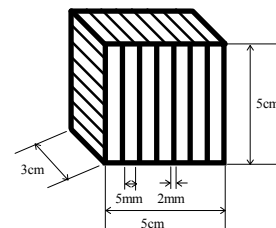


Figure 2 Box frame for groyne model

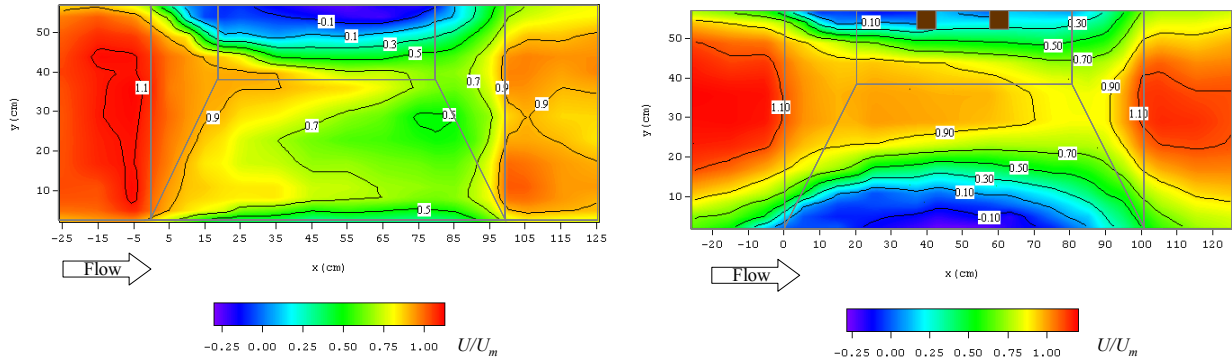


Figure 3 Contours of primary mean velocity in horizontal plane $z=5\text{cm}$, (left: Case SP, right: Case FP)

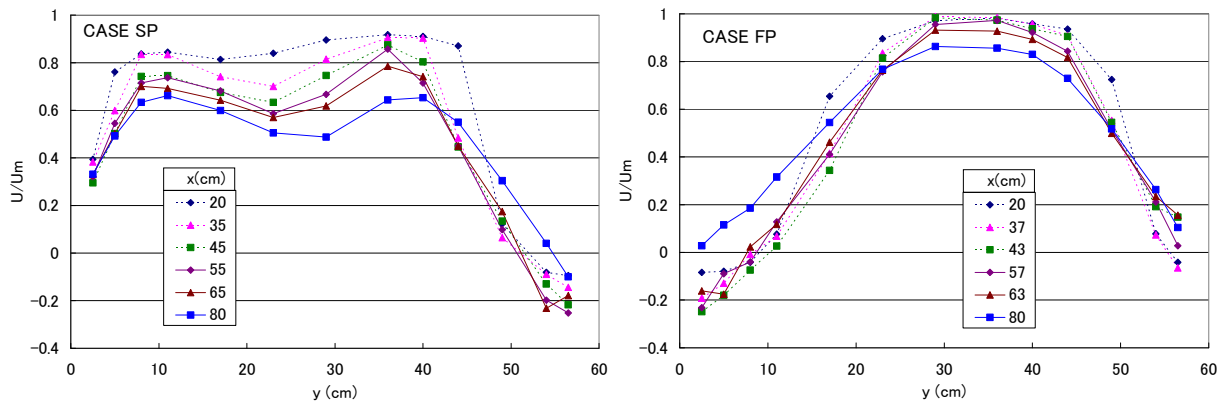


Figure 4 Lateral distribution of primary mean velocity at $z=5\text{cm}$ (left: Case SP, right: Case FP)

3. EXPERIMENTAL RESULTS AND DISCUSSION

Horizontal flow structures

Horizontal contours of primary mean velocity at $z=5\text{cm}$ are shown in Figure 3. The value is normalized by the bulk mean velocity U_m at $x=-25\text{cm}$. The primary velocity is decelerated where entering into the pool and is accelerated where going out from the pool. In the case SP, the velocity near the left-side wall in the deepest pool zone is significantly decelerated to show reverse velocity. A weak deceleration is observed at the right-side wall. As to the velocity in the central area, two penetrations of high velocity are recognized along the lines at $y=10\text{cm}$ and $y=35\text{cm}$. In the case FP, the deceleration area near the left-side bank is shrunk while large decelerated and reversed flow zone appears near the right-side wall. In this case, the central higher velocity zone is narrowed and single penetration of high velocity is observed. The deceleration in the downstream region of the pool becomes smaller.

Lateral distributions of U/U_m at $z=5\text{cm}$ are shown in Figure 4. The shape of distributions is extremely different from each other. In the case SP, the velocity in the deep-pool region is decelerated and twin peaks are observed clearly. The velocity in the side-slant region is rather accelerated as compared with the flow depth. In the case FP, the deceleration in the deep-pool region becomes smaller and the velocity in the side-slant region is much decelerated. Therefore, only one peak appear at about $y=30-35\text{cm}$.

Figure 5 shows horizontal velocity vectors at $z=5, 3$ and 1cm . In the case SP, a

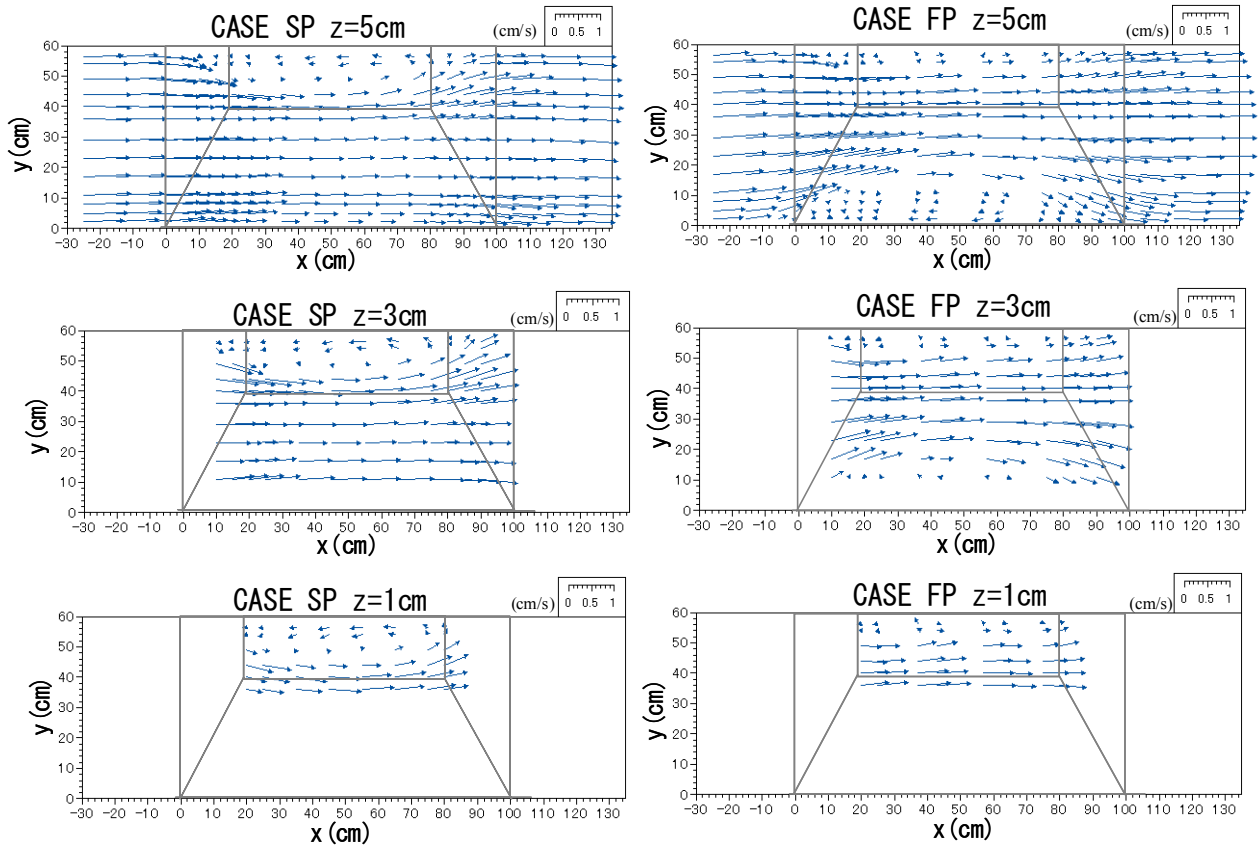


Figure 5 Velocity vectors in horizontal plane (left: Case SP, Right: Case FP)

separation vortex appears, attached on the left-side bank. The vortex is generated just on the flat area of the pool. This separation vortex shows cylindrical conformation without much change in size and strength from the bottom to the free surface. The flow is deflected toward the centre at the upstream slant of the pool and it is concentrated on the line of $y=40\text{cm}$. At the downstream slant of the pool, main flow turns back toward the left-side wall. Though there are no structures to make separation in the whole flow area, the separation vortex is generated. It is considered that the increased pressure in the deep pool zone induces the deflecting flow toward the channel centre. However, this mechanism has not been clearly explained yet. A small deceleration spot is observed along the right edge line of the side slant.

On the other hand, the flow pattern of the case FP is drastically different from that of the case SP. A large separation vortex observed in the case SP disappeared and the small vortices generated by groynes are observed in the flat area of the pool. Instead of this, a large separation vortex is generated, attached on the right-side bank. The size and strength of this vortex are almost similar to that of the left-pool vortex in the case SP. The box-type groynes restrain the generation of left-pool vortex attracting the main flow toward the left side and then the right-slant vortex develops. It is not easy to give a reasonable reason to express these phenomena at this time. It should be necessary to simulate the flow by using sophisticated numerical models.

Cross-sectional flow structures

Figure 6 shows the contours of primary mean velocity in the cross sections with (v, w) secondary-flow velocity vectors. In the entrance region of the pool ($x=10\text{cm}$), the downflow

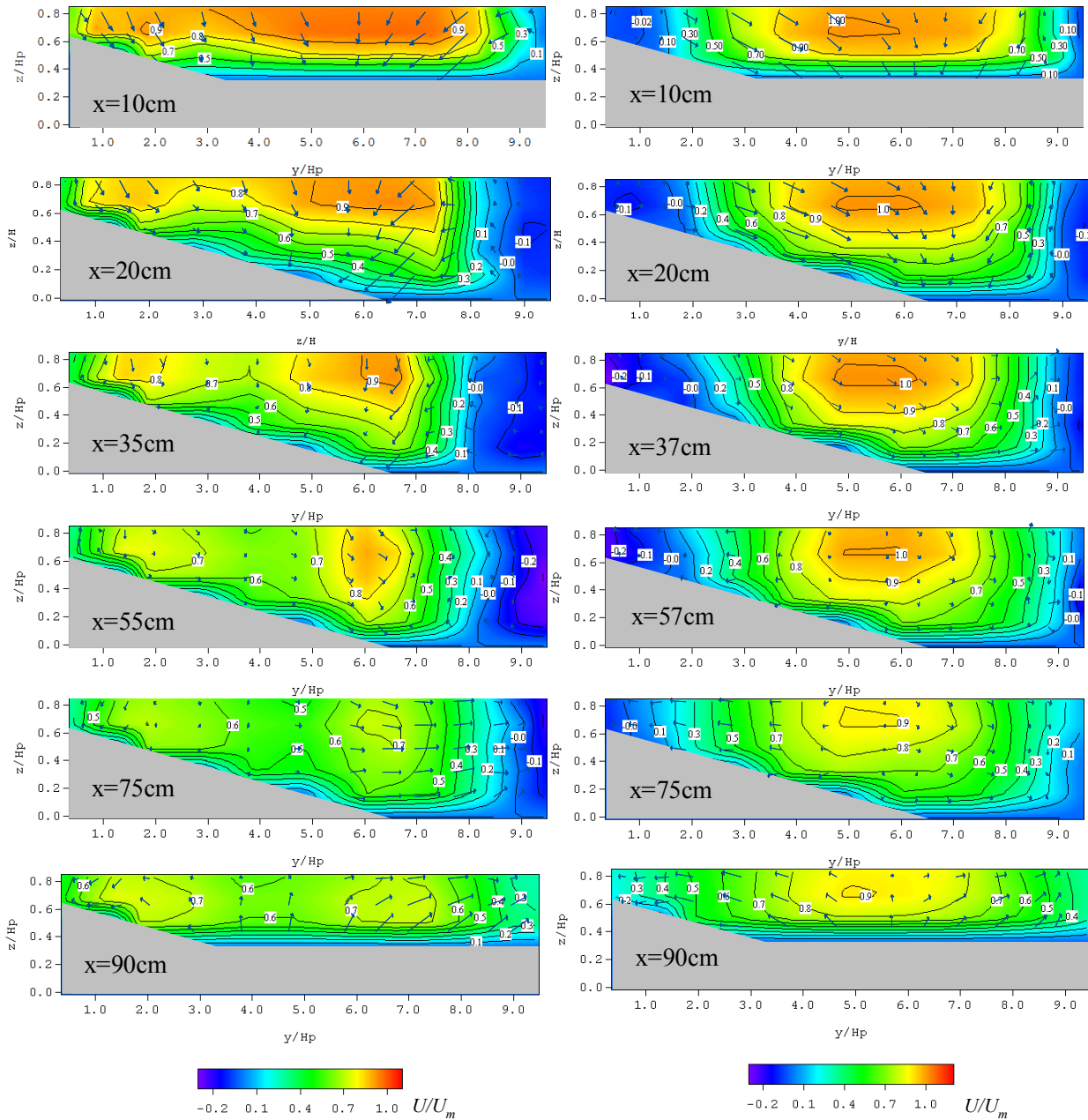


Figure 6 Contours of primary mean velocity in cross section
(left: Case SP, right: Case FP)

is significant. The downflow concentrates on two parts; $y/H_p=1.5 - 2.0$ and $y/H_p=6.0$, in the case SP, while the downflow is directed toward the down end of the side slant in the case FP. This tendency continues up to the end of front slant of the pool ($x=20\text{cm}$). On the flat region of the pool ($x=35\text{cm}$ to 75cm), twin peaks become remarkable in the case SP and high velocity areas are projected into near-bed region. These high velocity regions correspond well to the downflow regions. A decrease of velocity is noticeable in a half region of the deepest flat area, in the case SP. Contour lines adjacent to this low velocity zone distribute vertically and this part indicates a two-dimensional shear layer generated by the cylindrical vortex. In the case FP, a high velocity region appears at the central region ($y/H_p=5.0 - 6.0$) and the maximum velocity point appears below the free surface. A decrease of the velocity near the deep sidewall is not so large in comparison with the case SP, even though the groynes were

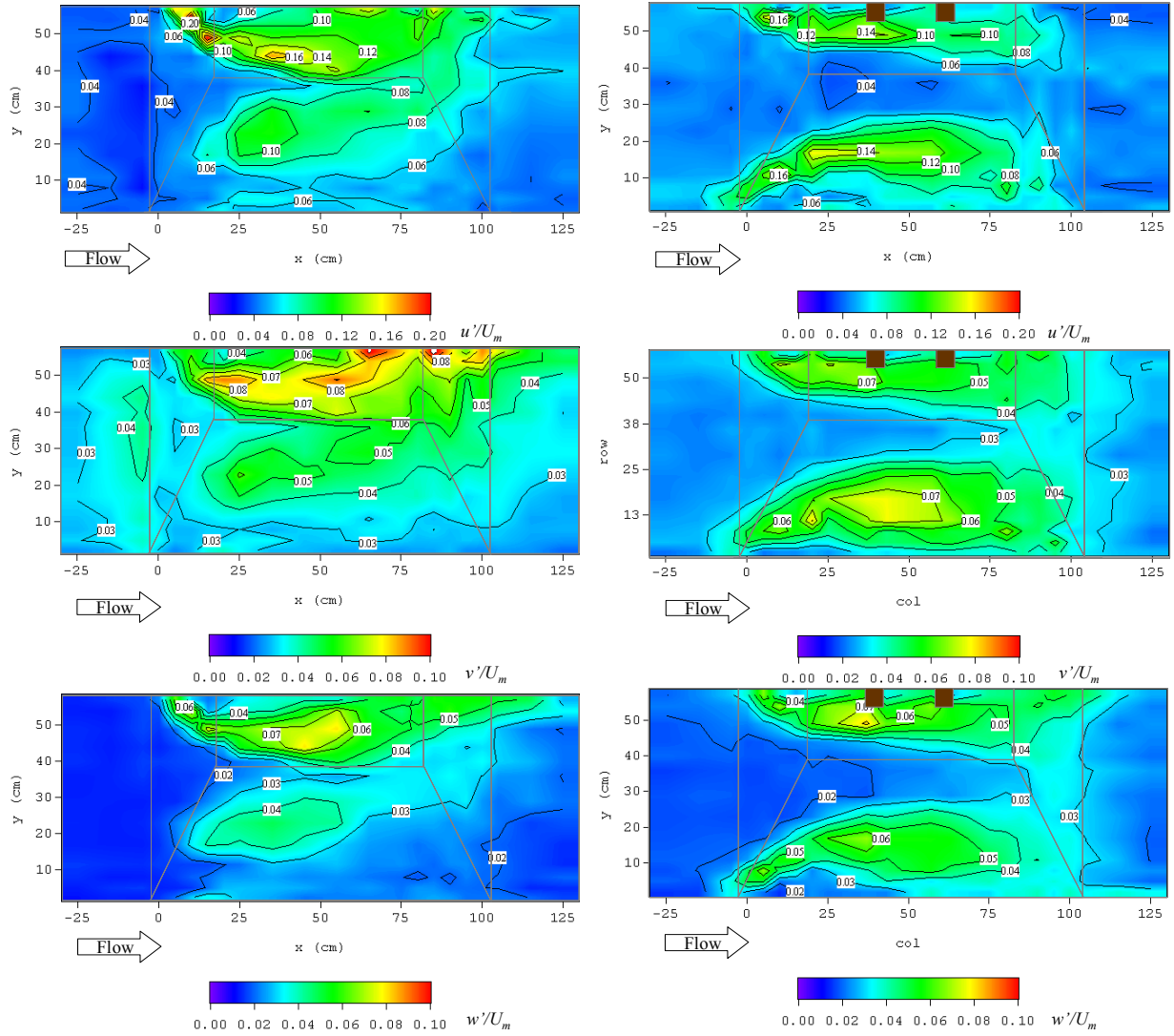


Figure 7 Contours of turbulence intensities in horizontal plane $z=5\text{cm}$
(left: Case SP, right: Case FP)

placed in the pool. On the other hand, a deceleration near the shallow sidewall becomes apparent in the case FP. At the tail region of the flat pool ($x=75\text{cm}$), a horizontal flow toward the deep wall appears in the case SP, while a horizontal flow toward the shallow side wall appears in the case FP. In the tail-slant region, the upflow is recognized and separated into both sidewalls in two cases. The feature of twin peaks maintained at this region in the case SP.

Turbulence characteristics

Figure 7 shows the contours of three components of turbulence intensity normalized by the mean velocity in horizontal plane of $z=5\text{cm}$. Turbulence intensities are increased along the interfacial region of the horizontal vortices observed in Figure 5. In the case SP, turbulence in the flat pool zone becomes noticeably large since deeper-side separation vortex structure is significant. A small maximum appears in the central region on the side slant. In the case FP, high turbulent regions are observed on both sides since the right-hand side is the separation vortex zone and the left-hand side is the groyne-induced retarded zone. The maximum values of turbulence intensities are larger in the case SP than those in the case FP.

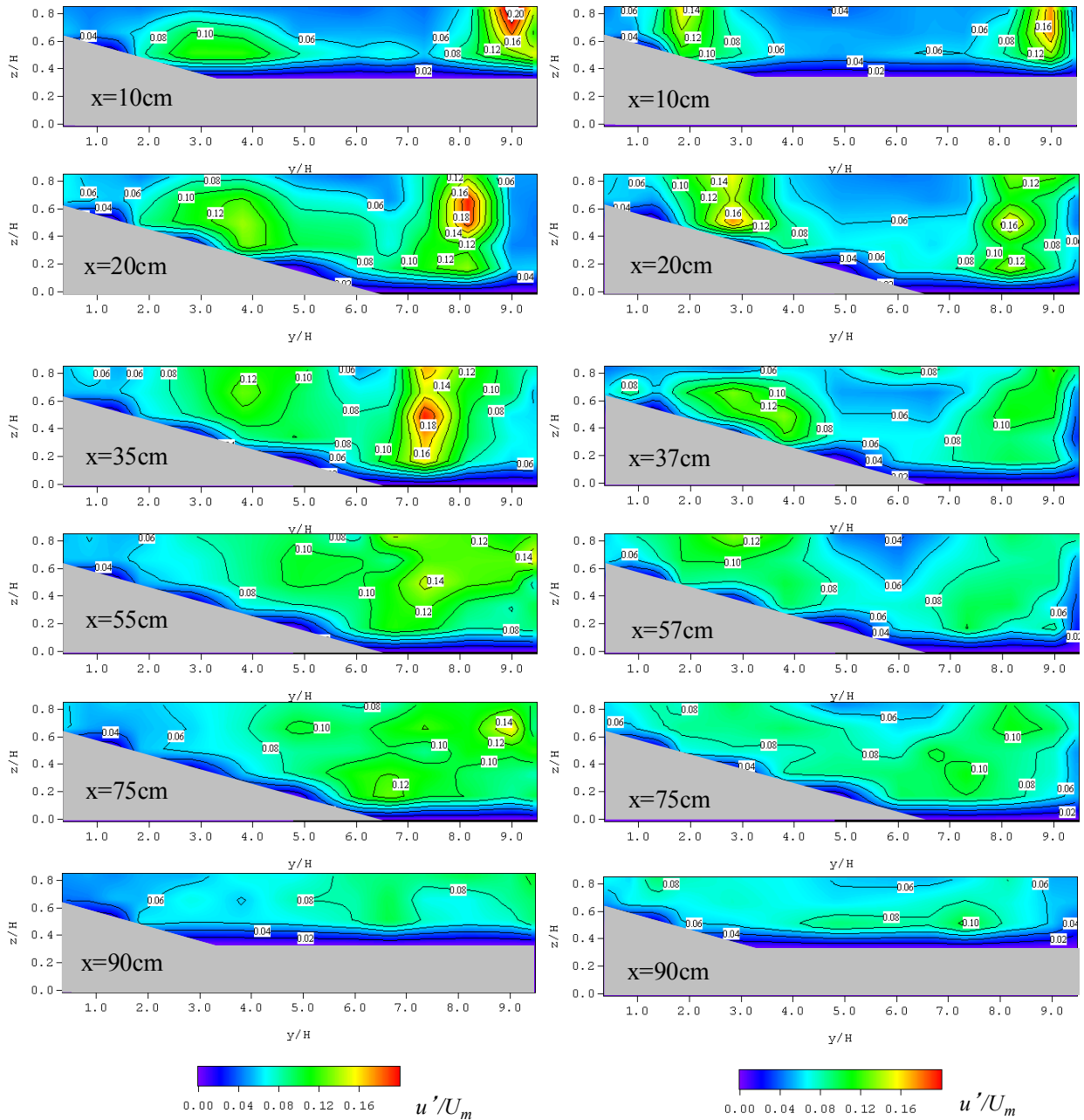


Figure 8 Contours of streamwise turbulence intensity in cross section (left: Case SP, right: Case FP)

The streamwise turbulence intensity, u' , becomes large in front of the vortex zone whereas the transverse turbulence intensity, v' , shows large value inside the vortex zone. The vertical turbulence intensity, w' , is large in the upstream-half region of the vortex zone.

Figure 8 shows the cross-sectional contours of streamwise turbulence intensity. In the case SP, it shows large peak value in the horizontal shear layer due to the large separation vortex from the entrance to the mid-section of the pool ($x=10\text{cm}$ to 35cm). In this longitudinal range, another small peak appear in the lateral range of $y/H=3.0 - 4.0$. This peak region corresponds to the intermediate zone between twin peaks of primary velocity. As going downstream from the mid-section of the pool, turbulence becomes to diffuse in the downstream-half region of the separation vortex. In the case FP, turbulence intensity attains maximum in the lateral shear layers on both sides in the upstream region of the pool ($x=10\text{cm}$

to 20cm) in the same manner as in the case SP. At the half section of the pool ($x=37\text{cm}$), the left peak region is stretched laterally and the right peak becomes obscure. In the downstream region of the pool, turbulence is decreasing and diffusing. Totally, turbulent structures are dominated by the horizontal vortices generated in the pool region.

4. CONCLUSIONS

Velocity measurements were conducted in the laboratory channel having a model pool with and without groynes. In this specific condition, a large separation vortex is generated in an asymmetric pool. This vortex characterizes the flow structures and turbulent structures in this flow field. The asymmetric pool arrangement may cause the lateral pressure gradient and then generates the separation vortex. This separation vortex is reproducible and definite phenomenon. It has not been verified by numerical simulations yet. It should be challenged by modellers by using 2-d and 3-d numerical models. On the other hand, when groynes are located in the flat pool region, the separation vortex in the deepest area is reduced in size and divided into small eddies around groyne structures. Alternately, A new separation vortex appears in the opposite side region on the side slant. The reason is considered the local acceleration due to the flow deflection by groynes but it is still not clear. These results do not give universal features of natural pool flows but give particular features of asymmetric pool arrangement in a straight channel. If the pool of this type is constructed in a straight river, it is not possible to maintain deep water-depth because of sand deposition. However, a combination of a pool and some obstacles such as groynes becomes to be useful for creating diverse flow conditions and for preventing a deep zone from deposition.

REFERENCES

- Booker, D. J., Sear, D. A., and Payne, A. J. (2002), Modelling three-dimensional flow structures and patterns of boundary shear stress in a natural pool-riffle sequence, *Earth Surf. Process Landforms* 26, pp553-576.
- Cui, Y., Wooster, K., Venditti, J. G., Dusterhoff, S. R., Dietrich, W. E. and Sklar, L. S. (2008), Simulating sediment transport in a flume with forced pool-riffle morphology: examinations of two one-dimensional numerical models, *J. Hydraulic Engineering, ASCE*, vol.134, No.7, pp.892-904.
- Miyamoto, H., Kanda, T. and Hyodo(2001), N.: Principal component analysis on turbulent structure in open-channel flow over concave bed, *Proc. of 29th Congress of IAHR, Theme D, Vol.1*, pp.21-27.
- Rodriguez, J. F., Garcia, M. H., Lopez, F. M. and Garcia, C. M. (2004), Three dimensional hydrodynamics of pool-riffle sequences for urban stream restoration, *River Flow 2004*, pp1297-1304.
- Seo, I. W., Hall, W and Maxwell, C. (1992), Modeling low-flow mixing through pools and riffles, *J. Hydraulic Engineering, ASCE*, vol.118, No.10, pp.1406-1423.